Biochemical and Biophysical Research Communications 461 (2015) 494–500

Contents lists available at ScienceDirect

Biochemical and Biophysical Research Communications

journal homepage: www.elsevier.com/locate/ybbrc

# Cavitation during the protein misfolding cyclic amplification (PMCA) method – The trigger for *de novo* prion generation?

Cathryn L. Haigh [a], Simon C. Drew [b, *]

[a] Department of Pathology, The University of Melbourne, Victoria 3010, Australia
[b] Florey Department of Neuroscience and Mental Health, The University of Melbourne, Victoria 3010, Australia

ARTICLE INFO

*Article history:*
Received 31 March 2015
Available online 17 April 2015

*Keywords:*
Prion
*de novo*
PMCA
Sonication
Cavitation
Free radical

ABSTRACT

The protein misfolding cyclic amplification (PMCA) technique has become a widely-adopted method for amplifying minute amounts of the infectious conformer of the prion protein (PrP). PMCA involves repeated cycles of 20 kHz sonication and incubation, during which the infectious conformer seeds the conversion of normally folded protein by a templating interaction. Recently, it has proved possible to create an infectious PrP conformer without the need for an infectious seed, by including RNA and the phospholipid POPG as essential cofactors during PMCA. The mechanism underpinning this *de novo* prion formation remains unknown. In this study, we first establish by spin trapping methods that cavitation bubbles formed during PMCA provide a radical-rich environment. Using a substrate preparation comparable to that employed in studies of *de novo* prion formation, we demonstrate by immuno-spin trapping that PrP- and RNA-centered radicals are generated during sonication, in addition to PrP-RNA cross-links. We further show that serial PMCA produces protease-resistant PrP that is oxidatively modified. We suggest a unique confluence of structural (membrane-mimetic hydrophobic/hydrophilic bubble interface) and chemical (ROS) effects underlie the phenomenon of *de novo* prion formation by PMCA, and that these effects have meaningful biological counterparts of possible relevance to spontaneous prion formation *in vivo*.



## 1. Introduction

Prions are proteinaceous infectious agents that cause transmissible neurodegenerative diseases such as Creutzfeldt Jakob Disease (CJD) and Bovine Spongiform Encephalopathy (BSE). Prion diseases are associated with the conversion of the normal structure of the prion protein ($PrP^{C}$) into an infectious conformer ($PrP^{Sc}$). $PrP^{Sc}$ accumulates in disease and provides a template for further $PrP^{C}$ misfolding and conversion.

The protein misfolding cyclic amplification (PMCA) technique is a cell-free method developed to amplify very small amounts of $PrP^{Sc}$. The process of PMCA involves "seeding" natively-folded $PrP^{C}$ (from whole brain, cell culture, or recombinant expression) with a minute quantity of infectious $PrP^{Sc}$, followed by repeated cycles of incubation and sonication [1]. A templating interaction with $PrP^{Sc}$ leads to the conversion of α-helical PrP to a β-sheet-rich protease-resistant $PrP^{res}$, whose properties are purported to be identical to those of brain-derived $PrP^{Sc}$. In this way, PMCA is viewed as a means to accelerate the conversion process that occurs *in vivo*, such that the presence of $PrP^{Sc}$ in the original titre can then be inferred by immunodetection of the amplified $PrP^{res}$.

Recently, the *de novo* generation of infectious PrP (ie. without addition of a $PrP^{Sc}$ seed) was reported by PMCA using only recombinant PrP (rPrP) expressed from *E. coli*, with RNA and the lipid POPG as essential cofactors [1–4]. Although it has been possible to propagate $PrP^{Sc}$ seeds using rPrP in the absence of RNA and POPG, both by PMCA [6,7] and vigorous shaking [8], the *de novo* generation of a recombinant PrP conformer that induces prion disease in wild type mice has only been demonstrated using PMCA in the presence of these cofactors [2–4]. The molecular mechanism underlying this phenomenon remains unknown.

Sonication of water at frequencies between 20 and 800 kHz causes a repeated expansion and collapse of microbubbles ("acoustic cavitation"). The extremely high local temperature and pressure

*Abbreviations:* PrP, prion protein; $PrP^{res}$, protease-resistant isoform of PrP; $PrP^{Sc}$, protease-resistant, infectious isoform of PrP; rPrP, bacterially expressed recombinant PrP; PMCA, protein misfolding cyclic amplification; DMPO, 5,5-dimethyl-1-pyrroline-N-oxide; DEPMPO, 5-(diethoxyphosphoryl)-5-methyl-1-pyrroline-N-oxide; 8OHdG, 8-hydroxyguanosine; EPR, electron paramagnetic resonance.

* Corresponding author. Postal address: Level 4, Kenneth Myer Building, Corner Royal Parade & Genetics Lane, The University of Melbourne, Victoria 3010, Australia. Fax: +61 3 9035 3107.
*E-mail addresses:* chaigh@unimelb.edu.au (C.L. Haigh), sdrew@unimelb.edu.au (S.C. Drew).

http://dx.doi.org/10.1016/j.bbrc.2015.04.048
0006-291X/

during cavitation leads to the splitting (sonolysis) of entrapped gaseous water molecules to form hydroxyl (·OH) and hydrogen (H·) radicals, in addition to downstream formation of hydrogen peroxide ($H_2O_2$) and superoxide radical anions ($\cdot O_2^-$) (Fig. 1A) [9,10].

In this study, we sought to determine whether bacterially-expressed PrP and any of its essential cofactors for *de novo* prion formation underwent observable free radical damage during PMCA. Using a combination of spin trapping, immuno-spin trapping and immunodetection of RNA oxidation, we identified the production of hydrogen, hydroxyl and superoxide radicals during PMCA, which caused protein-centred radicals, RNA-centred radicals and polypropylene-centred radicals, together with cross-linking of protease-resistant oxidised PrP-RNA adducts. This extensive free radical damage, in conjunction with cofactor interactions at the hydrophilic/hydrophobic interface of cavitation bubbles, may provide the necessary conditions for producing an oxidatively-modified conformer that subsequently acquires infectious properties.

## 2. Materials and methods

### 2.1. Reagents

Bovine serum albumin (BSA), 2-Oleoyl-1-palmitoyl-sn-glycero-3-phospho-rac-(1-glycerol) sodium salt (POPG) and phosphate-buffered saline (PBS; 10 mM phosphate, 2.7 mM KCl, 137 mM NaCl, pH 7.4) were purchased from Sigma–Aldrich. Thin-walled, RNAase-free 0.2 mL PCR tubes were obtained from Scientific Specialties Inc. Bacterially-expressed α-folded recombinant murine PrP(23–231) was obtained from Prionatis. Mouse Xpress Ref universal total RNA (whole body) was purchased from Qiagen. 5,5-dimethyl-1-pyrroline-N-oxide (DMPO) and 5-(diethoxyphosphoryl)-5-methyl-1-pyrroline-N-oxide (DEPMPO) were purchased from Alexis Biochemicals and used without further purification. Peroxide-free Triton X-100 (10% solution) was obtained from Amresco. Tris-buffered saline (10 ×, 100 mM Tris.HCl, 1.5M NaCl, pH 7.5) was obtained from G-BioSciences. RNase-free water was purchased from Qiagen. Rabbit polyclonal antibody directed against DMPO nitrone adducts was purchased from Abcam. The rabbit polyclonal antibody directed against residues 89–103 of mouse PrP (03R19) [11] was a kind gift of Dr Victoria Lawson (The University of Melbourne). Mouse monoclonal (clone 15A3) antibody directed against 8-hydroxyguanosine was obtained from Agrisera. Rabbit polyclonal antibody directed against methionine sulfoxide (MetO) was purchased from Cayman Chemical. HRP conjugated sheep anti-mouse and goat anti-rabbit IgG were purchased from GE Healthcare Lifesciences. ECL Select was obtained from Amersham. Proteinase K (Fungal) was purchased from Invitrogen. Water was "Milli-Q" grade (Millipore).

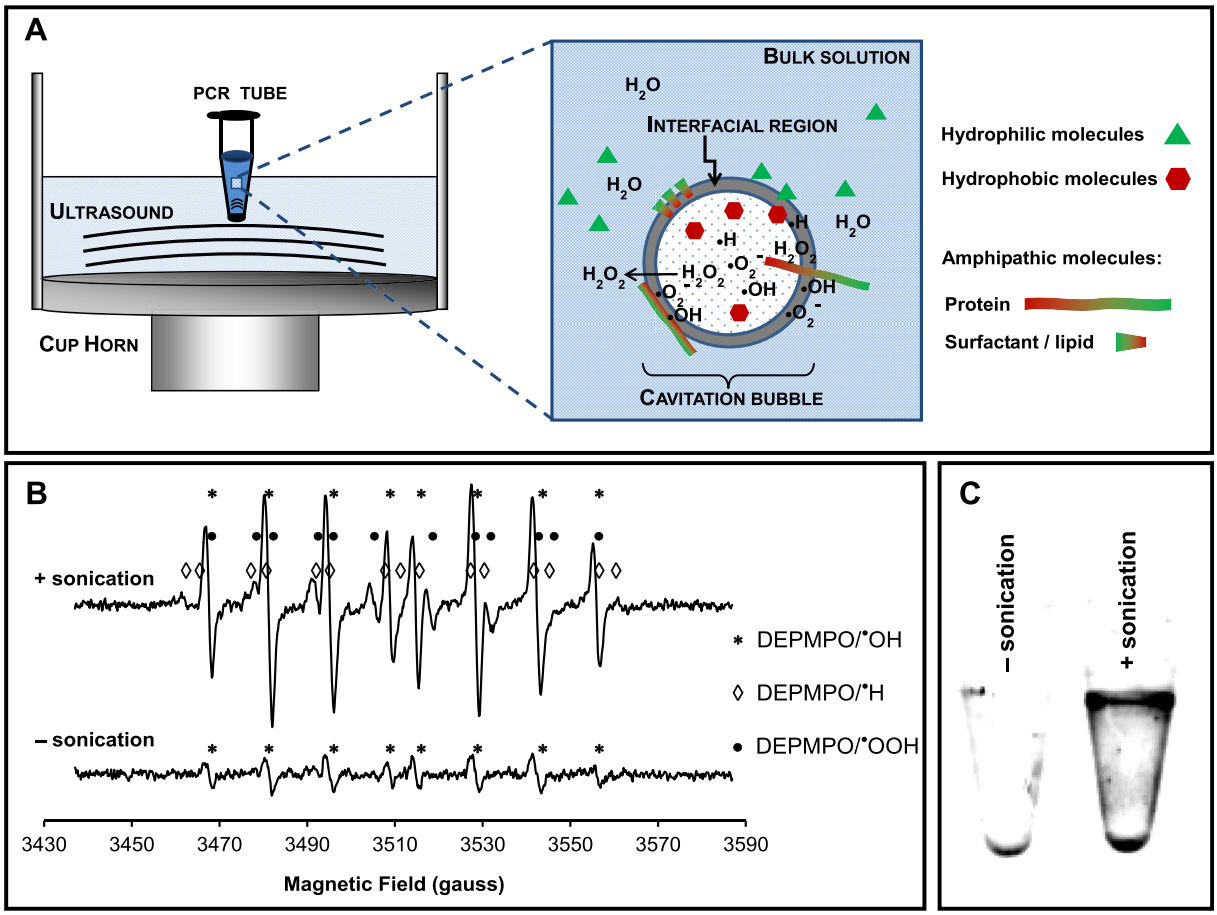


**Fig. 1.** (A) Schematic of sonochemical production of free radicals in solution. Radical reactions occur primarily within the hydrophobic interior of the gaseous bubble and at the bubble–water interface [10]. Surfactants have been shown to orient themselves radially at the gas–liquid interface of the cavitation bubble, with the polar head group facing the bulk aqueous environment [39] (B) After 5 min continuous 20 kHz sonication at 250 W, EPR spectroscopy of a PBS solution containing the spin trap DEPMPO shows the presence of multiplets of peaks that are diagnostic [40] of DEPMPO adducts with short-lived (·OH, asterisks) and hydrogen radicals (·H, diamonds), together with secondary superoxide radicals ($\cdot O_2^-$, filled circles). (C) DMPO immuno-spin trapping of radicals formed at the surface of polypropylene PCR tubes following 48 cycles of sonication (each cycle 30 s at 250 W every 30 min).

### 2.2. Sonication

Samples (100 μL) were contained in 200 μL thin-walled, flat cap, sterile polypropylene PCR tubes and placed in a Misonix Sonicator 4000 with cup-horn accessory and a perspex sample holder. The cup horn was filled with 200 mL distilled water and the tubes positioned such that the bottom of the PCR tube was 1–2 mm above the surface of the horn. A maximum of four tubes were sonicated at any one time. Each tube was placed near the centre of the sample holder and positioned such that no two tubes were immediately adjacent. Sonication at 20 kHz was and 250 W was carried out with an initial temperature of 23 °C.

### 2.3. PMCA

Sample preparation followed that used for *de novo* prion experiments [2,3] except for the conditional inclusion of the DMPO spin trap and the use of mouse universal total RNA in place of total RNA from mouse liver. The final reagent concentrations were: [PrP(23–231)] = 4.6 μg/mL (0.2 μM), [RNA] = 27 μg/mL, [POPG] = 4.0 μg/mL, [Triton X-100] = 4.3 mM (0.27%), [DMPO] = 100 mM, 10 mM Tris HCl, 150 mM NaCl, pH 7.5. Substrate was stored at −80° until use.

Each cycle of PMCA consisted of 30 s sonication at 250 W every 30 min. Each round of PMCA consisted of either 48 cycles (24 h) or 144 cycles (72 h). At the end of each round, 10 μL reaction product was added to 90 μL freshly thawed substrate. The sonicator was housed inside a dry incubator set at 37 °C. Control samples were incubated in the dark (to avoid breakdown of DMPO) without sonication at 37 °C.

### 2.4. Immunoblotting

Samples (2 μL) were spotted onto nitrocellulose (0.22 μm; Bio-Rad) and dried at 37 °C for 45 min. Unless otherwise stated, the membrane was blocked for 1 h at room temperature (RT) in PBST (10 mM PBS pH 7.5, 0.05% Tween-20) containing 5% w/v non-fat milk, antibody incubations were performed for 1 h at RT in PBST with 1% non-fat milk, wash steps after primary and secondary antibody incubations were carried out three times for 10 min in PBST. Antibody conjugates were detected by addition of ECL reagent and chemiluminescent imaging using a LAS-3000 imaging system (FujiFilm, Japan).

DMPO radical adducts were detected using anti-DMPO primary antibody (1:5000) and anti-rabbit HRP-conjugate secondary antibody (1:5000). PrP immunoblotting was performed using the 03R19 PrP antibody (1:5000) and anti-rabbit HRP conjugate (1:5000). Immunodetection of 8OHdG used anti-8OHdG antibody (1:2000) and anti-mouse HRP conjugate (1:5000). Oxidised methionine was detected using anti-MetO antibody (1:1000) following the manufacturer's instructions. Protease-resistance was determined by incubation of the membrane in PBST containing 100 μg/mL PK for 30 min at 37 °C in PK buffer (50 mM Tris HCl, 1 mM $CaCl_2$, pH 8.0), followed by denaturation in 3M GdnHCl for 10 min, rinsing in “Milli-Q” water 10 min, then immunoblotting as above.

For immunodetection of propylene-centred radicals, the DMPO solution in the PCR tube was discarded and the tube interior briefly washed three times (addition of 200 μL PBST, 5 s vortex mixing, and aspiration). The tubes were then treated in an identical manner to nitrocellulose membranes, except that the interior of the PCR tube was completely filled with block, anti-DMPO and anti-rabbit HRP antibody solutions. Wash steps were carried out by first aspirating the contents of the tube, followed by three brief PBST rinses as above, then additional immersion of the open tubes in PBST with gentle agitation for 30 min. The antibody conjugate was detected by filling each tube with a solution of ECL, incubating 2 min, then aspirating the bulk ECL and chemiluminescent imaging with the tube in the horizontal position.

### 2.5. EPR spectroscopy

To detect radical adducts, sonicated samples were immediately transferred to liquid nitrogen. Immediately before spectroscopic analysis, each sample was thawed and transferred to a quartz flat cell (Wilmad, WG-808-Q), which was positioned within a super-high-Q probehead (ER 4122SHQE) of an E500 X-band EPR spectrometer (Bruker). Continuous-wave EPR spectra were acquired at room temperature using the following parameters: microwave frequency, 9.86 GHz; microwave power, 10 mW, modulation amplitude, 1 G; receiver gain, 80 dB, receiver time constant, 40.96 ms; magnetic field sweep rate, 3.33 G/sec; 10 averages.

## 3. Results

### 3.1. PMCA provides a radical rich environment

The standard instrument for PMCA is the Misonix Sonicator 4000 with cup-horn accessory [1]. The frequency (20 kHz) and power (~1–3 Watts/$cm^3$) of sonication used for PMCA should be sufficient to trigger the free radical production (Fig. 1A). We first established that free radicals are produced under these conditions. To enable detection of these short-lived radicals, we used the spin trapping technique to form longer-lived radical adducts and then identified these adducts using electron paramagnetic resonance (EPR). One of the most widely used spin traps is DMPO that traps O-, N-, S-, and C-centred radicals. A closely related spin trap is DEPMPO, which forms longer-lived adducts with ·OH and $\cdot O_2^-$ radicals [12]. Using a solution of 100 mM DEPMPO, Fig. 1B demonstrates that the primary hydroxyl and hydrogen radicals produced by sonolysis can easily be detected after only a few minutes of sonication, in addition to secondary superoxide radicals. As expected, Fenton chemistry with trace levels of adventitious metal ions yields low levels of hydroxyl radical production without sonication.

The PMCA technique involves sonication of samples contained within 0.2 mL thin-walled polypropylene PCR tubes [1,2]. Hydroxyl radicals can abstract a hydrogen atom from polypropylene, which can further react with $O_2$ to form a peroxy radical that participate in further chain reactions with the polymer backbone or with other species in solution [13–15]. Therefore, we examined whether we could detect propylene-centred radicals using a novel immuno-spin trapping technique. In this method, the DMPO spin trap forms radical adducts that are subsequently detected using an antibody raised against DMPO [16–18]. The site of DMPO attachment is a specific marker for where the radical was formed. Fig. 1C shows that after discarding the DMPO solution and antibody binding to the interior surface, the PCR tube subjected to sonication yielded marked levels of DMPO reactivity, consistent with hydroxyl radical-mediated hydrogen atom abstraction from the polymer.

### 3.2. PMCA generates protein- and RNA-centred radicals

Hydroxyl radicals attack protein and nucleic acid by hydrogen atom abstraction to form carbon-centred radicals [19]. At typical protein concentrations employed in PMCA (<1 μM), EPR spectroscopy lacks the sensitivity to quantify the radical adducts formed by spin trapping. Therefore, we again employed the immuno-spin trapping method. To establish that free radicals produced by sonolysis of water lead to significant protein oxidation, we first

sonicated BSA solution in the presence of 100 mM DMPO, spotted the reaction product onto nitrocellulose a probed the membrane for DMPO adducts. Fig. 2 demonstrates that the production of protein-centred radicals monotonically increased as a function of both sonication time and protein concentration.

To demonstrate that typical PMCA substrates also undergo substantial oxidative modifications, we then prepared a reaction mixture identical to that used for the generation of *de novo* prions [2,3]. This reaction mixture included bacterially-expressed recombinant PrP23-231 and mouse total RNA. Samples were subjected to a single round of PMCA (144 cycles of 30 s sonication every 30 min). Control samples were incubated in the dark without sonication at 37 °C. To trap PrP- and RNA-centred radicals, we optionally included the spin trap DMPO at a concentration of 100 mM. At the completion of PMCA, the reaction products were spotted onto nitrocellulose and DMPO adducts were detected by immunoblotting. Significant immunoreactivity was only observed for the substrate subjected to PMCA and the signal was further seen to be specific for DMPO (Fig. 3A).

Nucleic acids do not bind to nitrocellulose unless immobilised by baking or UV cross-linking, but readily retained on the membrane if they are covalently cross-linked to protein [20,21]. Such cross-linking is possible following free radical damage to PrP and RNA [20]. The DMPO reactivity observed in Fig. 3A may therefore quantify the concentration of both PrP- and RNA-centred radicals. In this instance, PrP-RNA adducts would be expected to contain additional evidence of oxidative damage. To determine if PrP-RNA cross-links are generated during PMCA, we used the mouse monoclonal antibody raised against 8OHdG, a specific marker of RNA/DNA damage. Fig. 3B shows that RNA oxidation is detected, indicating that oxidatively-modified RNA is covalently cross-linked to the PrP bound to the membrane. As expected, the level of RNA damage during PMCA was lower in the presence of DMPO due to the spin trap's inherent radical scavenging property.

Next, we looked for evidence of PrP methionine oxidation using a polyclonal antibody directed against methionine sulfoxide (MetO). Fig. 3C shows that sonication during PMCA causes MetO formation. Interestingly, a higher MetO reactivity was observed in the presence of DMPO. This somewhat counter-intuitive result might be explained by the fact that the radical scavenging effect of DMPO prevents complete oxidation of methionine beyond MetO to the non-immunogenic sulfone form and/or that formation of DMPO adducts leads to alterations in Met residue surface exposure.

### 3.3. PMCA produces protease-resistant PrP that is oxidatively modified

Finally, we conducted PMCA experiments as above, except serial PMCA was performed, with each 24 h round comprising 30 s sonication every 30 min. At the end of each round, 10 μL reaction product was added to 90 μL fresh substrate. Fig. 4 shows that following PK digestion (100 μg/mL for 30 min at 37 °C), unsonicated controls were completely digested by PK. Samples subjected to serial PMCA retained protease-resistant PrP on the membrane and $PrP^{res}$ was further associated with DMPO reactivity, indicating that protease resistance is accompanied by free radical damage. It is noteworthy, however, that despite the some hydroxyl radicals being formed by trace metals in the absence of sonication (Fig. 1B), no PK resistance was observed in the absence of sonication (Fig. 4C). Whilst the formation of DMPO-PrP adducts at regions within the 03R19 epitope (residues 89–103) may reduce reactivity, there appeared to be less $PrP^{res}$ formed when serial PMCA was performed in the presence of DMPO. Less 8OHdG reactivity was evident during serial PMCA in Fig. 4 as compared with the single round in Fig. 3, which we attribute to the greater length (72 versus 24 h) of the PMCA round. Interestingly, no 8OHdG reactivity could be detected following PK digestion, both in the presence and absence of DMPO. This suggests that either no PrP-RNA cross-links were associated with $PrP^{res}$ or that $PrP^{res}$-RNA cross-links were present but contained no 8OHdG.

## 4. Discussion

Using a substrate preparation comparable to that employed in previous studies of *de novo* prion formation [2–4], the present data demonstrate that sonication during PMCA provides a

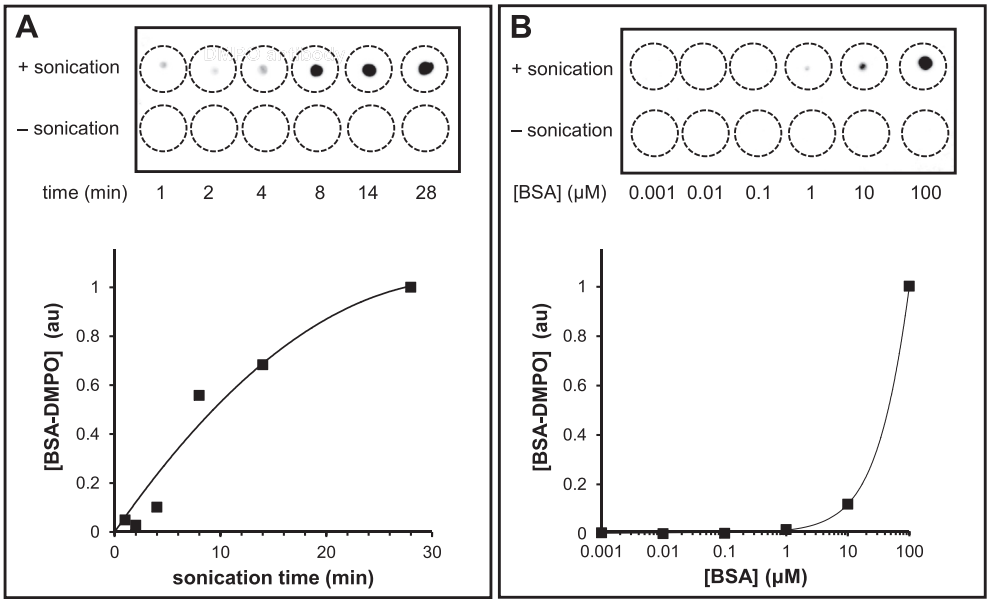


**Fig. 2.** Immuno-spin trapping analysis of protein-centred radical (DMPO/•BSA adduct) production during 20 kHz sonication at 250 W of a BSA solution in PBS containing 100 mM DMPO. Adduct concentration was measured (A) as a function of protein concentration (10 min sonication) and (B) as a function of sonication time (100 μM BSA).

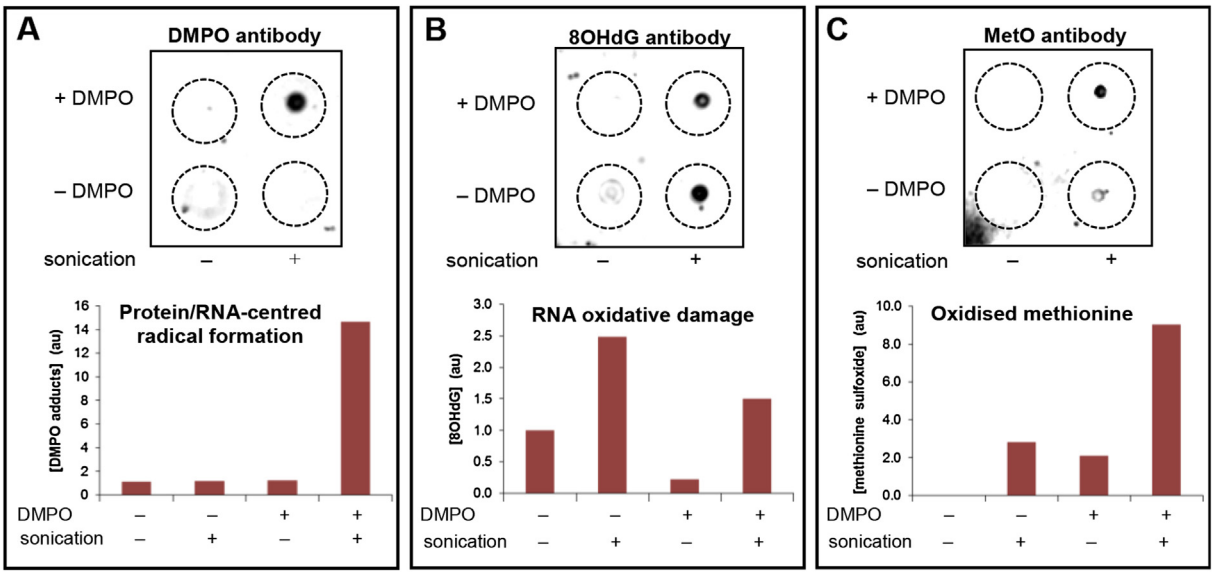


**Fig. 3.** Immuno-spin trapping analysis of PMCA reaction products (+sonication) and controls (−sonication) after one 72 h round of PMCA. Covalently cross-linked protein-RNA adducts containing (A) protein- and RNA-centred radicals (trapped by DMPO), (B) oxidative modification of RNA (8-hydroxyguanosine), and (C) oxidative modification of PrP (methionine sulfoxide) could be detected. Protein was spotted onto separate nitrocellulose membranes in A-C.

radical-rich environment that causes oxidation of protein and RNA, together with covalently cross-linked PrP-RNA adducts. Although the relevance to *de novo* prion formation remains unclear, we also observed radical damage to the polypropylene tubes in which the substrates were contained, which may also undergo cross-linking reactions with substrates. Importantly, we have established that PMCA generates PK-resistant PrP that is oxidatively modified and that inclusion of a radical scavenger such as DMPO appears to reduce $PrP^{res}$ formation. The absence of PK-resistant PrP cross-linked to 8OHdG-containing RNA (Fig. 4) following serial PMCA does not rule out $PrP^{res}$ cross-linking with RNA fragments containing adenosine. Indeed, *de novo* infectivity has also been demonstrated by PMCA using polyadenylic acid in place of total RNA [5]. We therefore cannot dismiss their role in *de novo* formation of an infectious particle during PMCA. Such a species is also not without biological relevance, since covalent protein-nucleic acid cross-links are known to be formed in the presence of hydroxyl radicals [20] and are also present in nature [22].

The widely-accepted view of the underlying mechanism of PMCA is that sonication provides a source of strong agitation that fragments the growing $PrP^{res}$ polymer into smaller pieces in order to expose $PrP^{C}$ to more "free ends" of misfolded $PrP^{res}$ [23]. Whilst it is true that large shear forces are generated during sonication that can lead to fragmentation [24], sonication also causes cavitation, with accompanying free radical production by sonolysis of water. In studies of the amyloidogenic PrP106–127 fragment, cavitation was proposed to promote stable β-sheet conformation and self-assembly at the boundary of the hydrophobic cavitation bubble interior and the hydrophilic bulk solution [25]. On the other hand, in quantitative investigations of the optimal ultrasonic power required for formation of amyloid fibrils from recombinant PrP, the vigorous agitation and very high local temperature and pressure was suggested to promote spontaneous nucleation of protein aggregates through increased probability of monomer association [28]. Undoubtedly, sonication can promote fibril formation, not only for PrP but also a number of other amyloidogenic proteins [26–29]. Nevertheless, in each of these instances, a major chemical phenomenon – the production free radicals during cavitation – was not considered. Although some studies unrelated to PMCA have speculated that $\cdot O_2^-$ may play a role in inter-protein disulfide cross-linking at the cavitation bubble interface [29,30], we are not aware of any prior direct demonstration of free radical damage to PrP during sonication, either as a trigger for (non-infectious) amyloid formation or *de novo* prion formation.

Earlier biochemical investigations have revealed that initial incubation with POPG during substrate preparation causes major rearrangements of PrP secondary structure, with successive addition of RNA exposing the N-terminus; these cofactor-induced structural features were found to persist in the infectious *de novo* $PrP^{Sc}$ conformer [31]. However, the requirement for sonication to create an infectious inoculum [2] indicates additional factors are required. Free radical production (eg. generated by $Fe^{II}/H_2O_2$) can oxidise PrP and generate β-sheet [32], but to our knowledge, *de novo* infectivity resulting from Fenton chemistry alone has never been demonstrated. Free radicals have been widely implicated in sporadic prion disease due to their ability to cause protein oxidation and misfolding [32–34], the observation of numerous markers of oxidative the stress in CJD brain [35], and the finding that PrP oxidation precedes $PrP^{Sc}$ formation in prion-infected brains [36,37]. We propose that the combined structural constraints imposed by the hydrophobic cavitation bubble and the production of free radicals at the bubble surface and interior may provide the optimal conditions for creating a synthetic prion.

Despite the seemingly artificial reaction conditions, the structural (membrane-mimicking interface) and chemical (ROS) environment present during PMCA has meaningful *in vivo* parallels. In line with the demonstration of polyadenylic acid as a minimal essential cofactor for recombinant PrP infectivity during PMCA [5], purinergic signalling also provides an abundant source of adenosine as an *in vivo* counterpart [38]. Therefore, PMCA should be viewed not only as tool to accelerate the *templating* interaction between $PrP^{C}$ and $PrP^{Sc}$ that occurs *in vivo*, but also as a means of mimicking ROS-mediated damage at biological membranes that may be responsible for initial $PrP^{Sc}$ *seeding* events. Further investigation of the inter-dependence of the above structural and chemical effects on *de novo* prion formation *in vitro* could yet

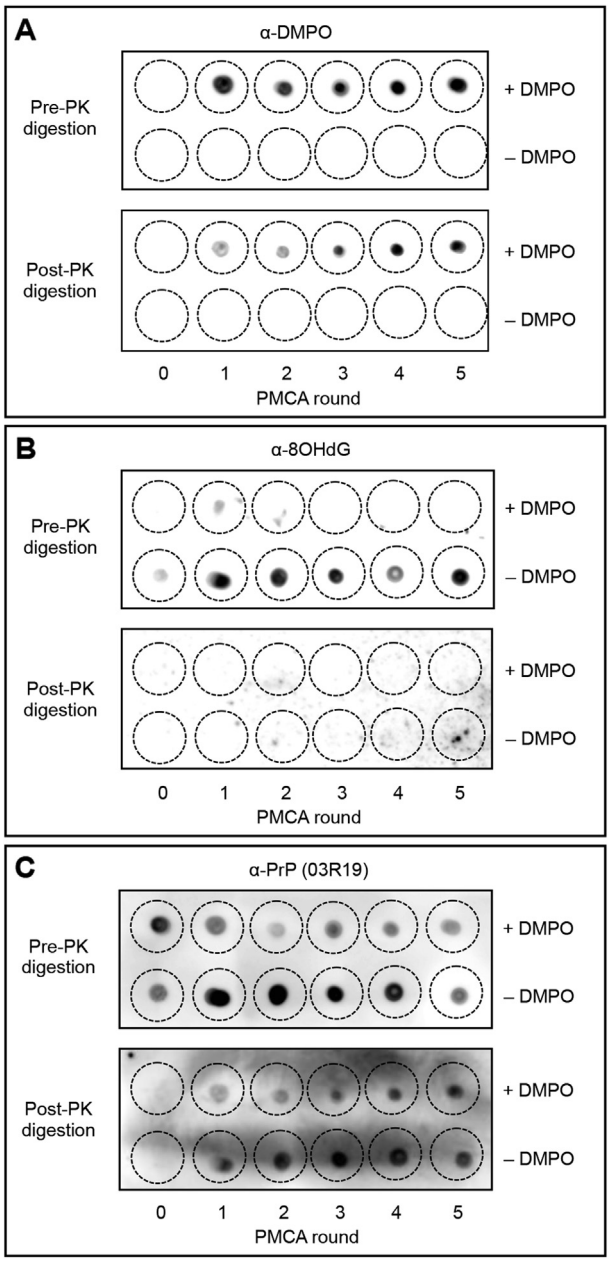


**Fig. 4.** Dot blot analysis of (A) DMPO, (B) 8OHdG and (C) PrP reactivity during serial PMCA (24 h per round), both pre- and post-PK digestion of the same membrane, showing the presence of PK resistant species ($PrP^{res}$) with DMPO reactivity. The membrane was stripped for 15 min in 1% HCl, before blocking and reprobing in *A–C*, first pre-PK and then post-PK digestion. The signal intensities before and after PK digestion are not directly comparable, since membrane digestion was followed by a GdnHCl denaturation step to promote $PrP^{res}$ epitope exposure.

provide useful insights into the triggers for sporadic prion disease *in vivo*.

## Conflict of interest

None.

## Acknowledgments

This work was supported by a Future Fellowship (FT110100199) awarded to S.C.D. and administered by the Australian Research Council.

## Transparency document

Transparency document related to this article can be found online at http://dx.doi.org/10.1016/j.bbrc.2015.04.048.

## References

[1] R. Morales, C. Duran-Aniotz, R. Diaz-Espinoza, M.V. Camacho, C. Soto, Protein misfolding cyclic amplification of infectious prions, Nat. Protoc. 7 (2012) 1397–1409.
[2] F. Wang, X. Wang, C.-G. Yuan, J. Ma, Generating a prion with bacterially expressed recombinant prion protein, Science 327 (2010) 1132–1135.
[3] F. Wang, X. Wang, J. Ma, Conversion of bacterially expressed recombinant prion protein, Methods 53 (2011) 208–213.
[4] Z. Zhang, Y. Zhang, F. Wang, X. Wang, Y. Xu, H. Yang, G. Yu, C. Yuan, J. Ma, De novo generation of infectious prions with bacterially expressed recombinant prion protein, FASEB J. 27 (2013) 4768–4775.
[5] F. Wang, Z. Zhang, X. Wang, J. Li, L. Zha, Genetic informational RNA is not required for recombinant prion infectivity, J. Virol. 86 (2012) 1874–1876.
[6] W.K. Surewicz, P. Gambetti, B. Caughey, R. Atarashi, B. Race, L. Qing, Q. Kong, G.J. Raymond, J.-I. Kim, I. Cali, K. Surewicz, Mammalian prions generated from bacterially expressed prion protein in the absence of any mammalian co-factors, J. Biol. Chem. 285 (2010) 14083–14087.
[7] N.R. Deleault, J.R. Piro, D.J. Walsh, F. Wang, J. Ma, J.C. Geoghegan, S. Supattapone, Isolation of phosphatidylethanolamine as a solitary cofactor for prion formation in the absence of nucleic acids, Proc. Natl. Acad. Sci. U. S. A. 109 (2012) 8546–8551.
[8] J.M. Wilham, C.D. Orrú, R.A. Bessen, R. Atarashi, K. Sano, B. Race, K.D. Meade-White, L.M. Taubner, A. Timmes, B. Caughey, Rapid end-point quantitation of prion seeding activity with sensitivity comparable to bioassays, PLoS Pathog. 6 (2010) e1001217.
[9] K. Makino, M.M. Mossoba, P. Riesz, Chemical effects of ultrasound on aqueous solutions. Formation of hydroxyl radicals and hydrogen atoms, J. Phys. Chem. 87 (1983) 1369–1377.
[10] N.H. Ince, G. Tezcanli, R.K. Belen, İ.G. Apikyan, Ultrasound as a catalyzer of aqueous reaction systems: the state of the art and environmental applications, Appl. Catal. B: Environ. 29 (2009) 167–176.
[11] V.A. Lawson, L.J. Vella, J.D. Stewart, R.A. Sharples, H. Klemm, D.M. Machalek, C.L. Masters, R. Cappai, S.J. Collins, A.F. Hill, Mouse-adapted sporadic human Creutzfeldt–Jakob disease prions propagate in cell culture, Int. J. Biochem. Cell. Biol. 40 (2008) 2793–2801.
[12] V. Roubaud, S. Sankarapandi, P. Kuppusamy, P. Tordo, J.L. Zweier, Quantitative measurement of superoxide generation using the spin trap 5-(Diethoxyphosphoryl)-5-methyl-1-pyrroline-N-oxide, Anal. Biochem. 247 (1997) 404–411.
[13] F. Posada, P. Malfreyt, J.-L. Gardette, Hydrogen abstraction from poly(-propylene) and poly(propylene oxide) by hydroxyl radicals: a computational quantum semi-empirical study, Comput. Theor. Polym. Sci. 11 (2001) 95–104.
[14] B. Ranby, J.F. Rabek, Photodegradation, Photo-oxidation and Photo-stabilization of Polymers: Principles and Applications, John Wiley & Sons, London, 1975.
[15] G. Geuskens, C. David, The photooxidation of polymers. A comparison with low molecular weight compounds, Pure Appl. Chem. 51 (1979) 233–240.
[16] D.C. Ramirez, S.E.G. Mejiba, R.P. Mason, Copper-catalyzed protein oxidation and its modulation by carbon dioxide, J. Biol. Chem. 280 (2006) 27402–27411.
[17] D.C. Ramirez, R.P. Mason, Immuno-spin trapping: detection of protein-centered radicals, Curr. Protoc. Toxicol. 24 (2005), 17.7.1–17.7.18.
[18] S.E. Gomez-Mejiba, Z. Zhai, H. Akram, L.J. Deterding, K. Hensley, N. Smith, R.A. Towner, K.B. Tomer, R.P. Mason, D.C. Ramirez, Immuno-spin trapping of protein and DNA radicals: "Tagging" free radicals to locate and understand the redox process, Free Radic. Biol. Med. 46 (2009) 853–865.
[19] B.S. Berlett, E.R. Stadtman, Protein oxidation in aging, disease, and oxidative stress, J. Biol. Chem. 272 (1997) 20313–20316.
[20] H. Schuessler, E. Jung, Protein-DNA-crosslinks induced by primary and secondary radicals, Free. Rad. Res. Comms 6 (1989) 161.
[21] P.S. Thomas, Hybridisation of denatured RNA and small DNA fragments transferred to nitrocellulose, Proc. Natl. Acad. Sci. U. S. A. 77 (1980) 5201–5205.
[22] Y.F. Drygin, Natural covalent complexes of nucleic acids and proteins: some comments on practice and theory on the path from well-known complexes to new ones, Nucleic Acids Res. 26 (1998) 4791–4796.
[23] K.S. Lee, B. Caughey, A simplified recipe for prions, Proc. Nat. Acad. Sci. U. S. A. 104 (2007) 9551–9552.
[24] M.T. Taghizadeh, A. Mehrdad, Calculation of the rate constant for the ultrasonic degradation of aqueous solutions of polyvinyl alcohol by viscometry, Ultrason. Sonochem 10 (2003) 309–313.
[25] K.S. Satheeshkumar, R. Jayakumar, Sonication induced sheet formation at the air–water interface, Chem. Commun. (2002) 2244–2245.
[26] O.M.A. El-Agnaf, G.B. Irvine, D.J.S. Guthrie, Conformations of β-amyloid in solution, J. Neurochem. 68 (1997) 437–438.
[27] Y. Ohhashi, M. Kihara, H. Naiki, Y. Goto, Ultrasonication-induced amyloid fibril formation of 2-Microglobulin, J. Biol. Chem. 280 (2005) 32843–32848.

[28] K. Yamaguchi, T. Matsumoto, K. Kuwata, Proper calibration of ultrasonic power enabled the quantitative analysis of the ultrasonication-induced amyloid formation process, Prot. Sci. 21 (2012) 38–49.
[29] P.B. Stathopulos, G.A. Scholz, Y.-M. Hwang, J.A.O. Rumfeldt, J.R. Lepock, E.M. Meiering, Sonication of proteins causes formation of aggregates that resemble amyloid, Prot. Sci. 13 (2004) 3017–3027.
[30] M.W. Grinstaff, K.S. Suslick, Air-filled proteinaceous microbubbles: synthesis of an echo-contrast agent, Proc. Natl. Acad. Sci. U. S. A. 88 (1991) 7708–7710.
[31] M.B. Miller, D.W. Wang, F. Wang, G.P. Noble, J. Ma, V.L. Woods Jr., S. Li, S. Supattapone, Structure 21 (2013) 2061–2068.
[32] N.D. Younan, R.C. Nadal, P. Davies, D.R. Brown, J.H. Viles, Methionine oxidation perturbs the structural core of the prion protein and suggests a generic misfolding pathway, J. Biol. Chem. 287 (2008) 28263–28275.
[33] D.B. Oien, T. Canello, R. Gabizon, M. Gasset, B.L. Lundquist, J.M. Burns, Ja Moskovitz, Detection of oxidized methionine in selected proteins, cellular extracts and blood serums by novel anti-methionine sulfoxide antibodies, Arch. Biochem. Biophys. 485 (2009) 35–40.
[34] M.I.Y. Elmallah, U. Borgmeyer, C. Betzel, L. Redecke, Impact of methionine oxidation as an initial event on the pathway of human prion protein conversion, Prion 7 (2013) 1–8.
[35] M. Freixes, A. Rodríguez, E. Dalfó, I. Ferrer, Oxidation, glycoxidation, lipoxidation, nitration, and responses to oxidative stress in the cerebral cortex in Creutzfeldt-Jakob disease, Neurobiol. Aging 27 (2006) 1807–1815.
[36] T. Canello, R. Engelstein, O. Moshel, K. Xanthopoulos, M.E. Juanes, J. Langeveld, T. Sklaviadis, M. Gasset, R. Gabizon, Methionine sulfoxides on $PrP^{Sc}$: a prion-specific covalent signature, Biochemistry 47 (2008) 8866–8873.
[37] T. Canello, K. Frid, R. Gabizon, S. Lisa, A. Friedler, J. Moskovitz, M. Gasset, R. Gabizon, Oxidation of Helix-3 methionines precedes the formation of PK resistant $PrP^{Sc}$, PLoS Pathog. 6 (2010) e1000977.
[38] G. Burnstock, Introduction to purinergic signalling in the brain, in: J. Barańska (Ed.), Glioma Signaling, Advances in Experimental Medicine and Biology, 986, Springer, Dordrecht, 2013, pp. 1–12.
[39] A.E. Alegria, Y. Lion, T. Kondo, P. Riesz, Sonolysis of aqueous surfactant solutions, probing the interfacial region of cavitation bubbles by spin trapping, J. Phys. Chem. 93 (1989) 4908–4913.
[40] B. Kukavica, M. Mojović, Ž. Vučinić, V. Maksimović, U. Takahama, S.V. Jovanović, Generation of hydroxyl radical in isolated pea root cell wall, and the role of cell Wall-Bound peroxidase, Mn-SOD and phenolics in their production, Plant Cell. Physiol. 50 (2009) 304–317.